Image Quality in Digital Radiography.
First Results of an analytical modeling approach.

Vasiliki A. Spyropoulou[1], Nektarios Kalyvas[1,2], Anastasios Gaitanis[1,2], Ioannis S. Kandarakis[2*], George S. Panayiotakis[1]

[1]*Department of Medical Physics, Medical School, University of Patras, 265 00 Patras, Greece*
[2]*Department of Medical Instruments Technology, Technological Educational Institution of Athens, Ag. Spyridonos, Aigaleo, 122 10 Athens, Greece*

* Corresponding author: kandarakis@teiath.gr

Abstract. *Any X-ray detector for medical imaging needs to serve the purpose of efficiently absorbing the impinging X-ray flux and converting it into a geometry-conserving digital image signal. The detector used should be optimized for each X-ray imaging modality. The aim of this work was to develop an analytical model simulating an indirect flat panel digital detector which could be later utilized in Computed Tomography Breast Imaging and to evaluate 2-dimensional images produced by irradiating a software phantom consisting of different orthogonal structures (tumor and microcalcifications). The detector was modeled within the framework of the linear cascaded systems (LCS) theory. The image unsharpness as well as the statistical noise, where post introduced in the final image, by utilizing the Transfer Function and the Noise Power Spectrum derived from the LCS model. Phantom images of various exposures conditions were derived. It was observed that the structures of the phantom were more visible as the kV and tissue thickness increased. Finally the microcalcifications were distinguished more easily than the tumors.*

Keywords: Flat panel; Indirect detector; Linear cascaded systems theory; Image quality;

1 Introduction

An X-ray medical imaging detector needs to serve the purpose of efficiently absorbing the impinging X-ray flux and converting it into a geometry-conserving digital image signal. The spatial resolution of the detector should be selected to meet the requirements of the respective application. While the signal per absorbed X-ray should be maximized, the noise introduced by the numerous conversion and amplification steps is required to be kept at a minimum [1] so as to optimize the signal-to-noise ratio.

Currently available flat panel detector technology covers X-ray medical imaging applications ranging from general radiography to computed tomography. The commercially available detectors are either convert the of X-ray quanta into electric charge directly, or use a scintillator screen as an interface, where the X-ray radiation is converted into light which in turn is absorbed, creating electric charge (indirect detection) [1]. Flat-panel imagers typically use a layer of either amorphous silicon (*a*-Si) [2] or amorphous selenium (*a*-Se) photodiodes to convert photons to electric charge. Due to its high atomic number and density, *a*-Se is suitable for direct detection of x rays. *a*-Si is typically combined with a scintillator to convert x-ray photons to optical photons that are efficiently absorbed by the silicon. Terbium-doped

gadolinium oxysulphide (Gd$_2$O$_2$S:Tb) and thallium-doped cesium iodide (CsI:Tl) are the most commonly used scintillators for this purpose due to their high atomic number, density, and light yield [3]. Active-matrix flat panel imagers (AMFPIs) contain an array of thin-film transistors, usually fabricated from *a*-Si, to address the photodiode array. Charge is read out one row at a time to a set of preamplifiers and analog to digital converters (ADCs) [4].

Modeling of imaging detectors is reported in literature [4-6]. These models are either using MONTE CARLO methodology [5] or the Linear Cascaded Systems approach [6-8]. The latter is well documented Cunningham 1998 [8] and has been applied by Kalivas et al [9] Siewerdsen et al (1996) [6] and Jee et al (2003) [7] to study phosphor based imaging detectors, x-ray digital radiography and digital mammography detectors. X-ray imaging simulation is also reported in literature either by Monte Carlo methodology[10].

In this study a theoretical model was created for the simulation of an indirect flat panel detector. In particular a CsI:TI scintillator deposited on an a-Si:H active matrix photodiode-TFT array was considered. For the evaluation of the detector performance and the derivation of its corresponding image quality parameters (Signal Power Spectrum and Noise Power Spectrum) the linear cascaded systems theory was applied [7]. In addition a simple, pixelized software phantom with orthogonal structures corresponding to breast tumor and microcalcifications was considered. The phantom was assumed to be irradiated with X-ray photons with energies corresponding to X-ray radiography. The transmitted X-ray fluence from the phantom, corresponding to subject contrast, was detected by the indirect flat panel detector and presented as a "detected" digital image. In addition the model predicted detector noise and unsharpness properties were used to post process the "detected" image and a final image was derived. In this work the preliminary results of this study are presented.

2   Materials and methods

In this study a theoretical model was developed in a Matlab platform for the evaluation of images derived from the simulation. The model assumes an input of X-ray quanta of energy E and predicts the output in terms of: mean signal value, modulation transfer function (MTF) and noise power spectrum (NPS). The images were obtained by creating a software phantom, consisting of different microcalcification and/or tumor sizes and irradiating it with monoenergetic energy beams corresponding to the mean energy of 70, 80, 90 and 100 kVp X-ray spectra. The software phantom was a 2-dimension matrix of 128 elements (128x128) and to each pixel the linear attenuation coefficients of tissue, microcalcification or tumor was assigned. Then, the irradiated image was inserted in the simulated flat panel detector and the final image occurred was the one that was evaluated.

The detector was considered to be an indirect detector, particularly CsI:TI coupled with a: Si-H photodetectors. The thickness of CsI:TI was 60mg/cm^2, the pixel area was 400 mm x 300 mm and the pixel dimension was 194 μm [11]. The detector was modeled, based on the linear cascaded systems theory [7-8][12-14].The latter was represented as a series of cascaded signal amplification and/or signal blurring stages. Each stage represents a physical wide sense stationary (WSS) process [7] that governs the transfer of signal and noise from the input to the output of the cascaded stages [6]. For these stages some assumptions were taken under consideration, these are: a) the MTF of a structured phosphor, like the needle-like shaped crystals of CsI, is

comparable to that of a powder phosphor screen of half the thickness[15]. Thus, the analytical models established for powder phosphors [9,16] can be used for structured phosphors provided the effective thickness is modified appropriately [9], b) a proportion of 1:1 between captured optical photons and generated e-h pairs was assumed [6], c) spreading of electron-hole pairs was assumed to be negligible [6,17].

The optical parameters of the scintillator used in the simulation were taken from literature [9,16]. The percentage of the optical photons coming out of the CsI:TI and being detected from the amorphous silicon (a:Si) depends on the spectral matching factor which took the value of 0.8 [9]. Additionally a fill factor, which gives the percentage of pixel area that is fulfilled by the area of the photodiode, took the value of 0.7 [11]. Finally, the additive electronic noise of the system was considered to be 1000e- [18].

The quantum noise and the light blur influence on the final image were considered as a post process function. The noise was assumed to follow a normal distribution and was added in the derived image. The parameters of the normal distribution mean signal value and signal variance deviation were calculated by the LCS detector modeling. In particular the signal variance was calculated as: [19]:

$$\sigma^2 = \sum_0^u NPS(u) \qquad (1)$$

The spatial resolution of an imaging system or component is often characterized by measuring the MTF in the frequency domain or the PSF in the spatial domain. The overall MTF of a cascaded imaging system is the product of the MTFs for individual stages. In the spatial domain, the overall PSF is the convolution of the PSFs for individual stages. In the detector, the light photons converted from the x-ray photons are scattered in all directions and the resulting light intensity signals spread out away from the incident point. The PSF for this signal spread may be approximated by a 2D Gaussian function as follows [20]:

$$G_S(x,y) = \frac{1}{2\pi\sigma_S^2} \exp\left(-\frac{x^2 + y^2}{2\sigma_S^2}\right) \qquad (2)$$

Where σ_s is the variance of the Gaussian function. In order to estimate σ_s, the transfer function corresponding to equation (2) was calculated and compared with the MTF derived from the analytical model. Finally, a 5x7 PSF table was created around the maximum value and was incorporated in the image taken from the detector.

3   Results and discussion

Figure 1 shows the Modulation Transfer Function (MTF) derived from the system and the one derived from equation (2). Best match was found for σ_s equals 2. .
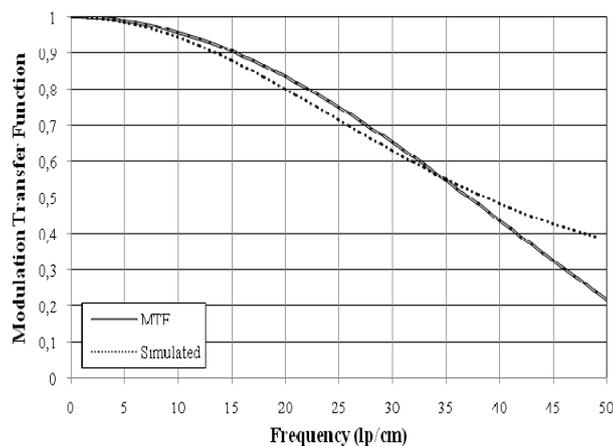
Figure 1. MTF of the model and the simulated for 70kVp.

In fig.2 it is shown the software phantom before the irradiation. It can be seen that on the right side of the image the microcalcification sizes are smaller while on the left side of the image are bigger.
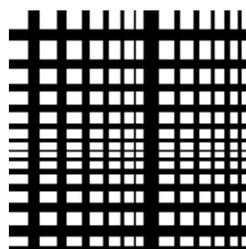
Figure 2. Initial image of the phantom before the irradiation.

In fig.3 (a and b) two images of the phantom for 14 cm tissue thickness and 0.02cm microcalcification thickness are shown. The first was irradiated with 70kV and the second with 100kV. It is shown that in the image corresponding to 100kV the microcalcification structures are more visible.

.

(a)   (b)
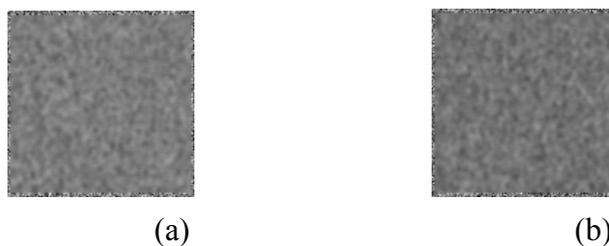
Figure 3. Images taken at the output of the detector for 14 cm tissue thickness, 0.02 cm microcalcification thickness and 70 and 100 kV respectively.

In fig. 4a,b,c three phantom images for 14 cm tissue thickness, 70 kV and

different microcalcification thickness (0.005cm, 0.02cm and 0.08cm respectively) are presented. It can be seen that as the sizes of microcalcification increases, the structures are more distinctive..

(a)   (b)   (c)
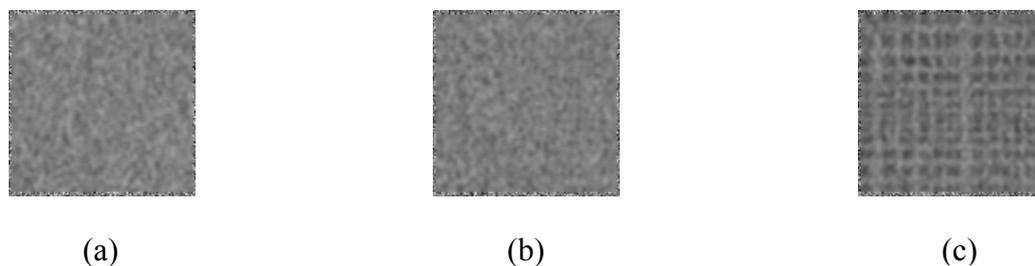
Figure 4. Images taken at the output of the detector for 14cm tissue thickness, 70 kV and
0.005, 0.02 and 0.08 cm microcalcification size respectively.

Fig. 5a and Fig 5b shows images of 12cm tissue thickness, 0.08 cm microcalcification thickness and different energy value, 80 and 90 kV respectively. The second picture is slightly worse than the first one, especially in the centre of the image where the structures of the phantom are closely to each other. That means that for the 12 cm tissue thickness as the x-ray tube voltage decreases the resolution of the system is better and can distinguish structures close to each other.

(a)   (b)

Figure 5. Images taken at the output of the detector for 12cm tissue thickness, 0.08cm microcalcification thickness and 80 and 90kV respectively.

In the following figure (Fig. 6a,b) two images for 100kV, 0.08cm microcalcification thickness and 12 and 14cm tissue thickness are presented. As the tissue thickness increases, with stable microcalcification thickness and x- ray tube voltage, the structures contained in the phantom are more visible.

(a)   (b)
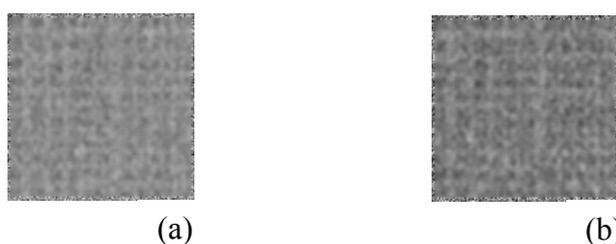
Figure 6. Images taken at the output of the detector for 100 kV, 0.08 cm microcalcification thickness and 12 and 14 cm tissue thickness respectively.

In the following figure (Fig.7a,b) two images for 90kV, 14cm tissue thickness and 0.02cm tumor and microcalcification thickness are demonstrated. It can be seen that the microcalcifications in Fig 7b are better visualized than the tumor in figure 7a

(a)   (b)

Figure 7. Images taken at the output of the detector for 90kV, 14cm tissue thickness and 0.02 cm tumor (a) and microcalcification (b) thickness respectively.

4   Conclusions

A theoretical model was developed to simulate the operation of an indirect flat-panel detector. For this purpose a software phantom was created with different sizes of microcalcification or tumors and it was irradiated. It was found that as the microcalcification thickness increases the images are more visible. Also, as the thickness of the tissue decreases the structures are less visible because they are very close to each other and the system does not separate them easily as different structures. Finally, microcalcifications are more visible than tumors. Future work of the present study is to create a better and more realistic phantom and to perform evaluation of the images taken from the model.

REFERENCES

[1]   Spahn Martin (2005), " Flat detectors and their clinical applications", *Eur. Radiol., Vol. 15*, pp. 1934-1947.

[2]   J. H. Siewerdsen, L. E. Antonuk, Y. El-Mohri, J. Yorkston, W. Huang, and I. A. Cunningham (1998), "Signal,   noise power spectrum, and detective quantum efficiency of indirect-detection flat-panel imagers for diagnostic radiology" *Med. Phys. Vol.25*, pp.614-628.

[3]   C. W. E. van Eijk (2002), "Inorganic scintillators in medical imaging", *Phy. Med. Biol., Vol.47*, pp.85-106.

[4]   J. C. Blakesley, R. Speller (2008), "Modeling the imaging performance of prototype organic x-ray imagers", *Med. Phys., Vol. 35(1)*, pp. 225-239.

[5]   Liaparinos F.P. and Kandarakis S. I. (2009), "The Monte Carlo evaluation of

noise and resolution properties of granular phosphor screens″, *Phys.Med.Biol.*, *Vol.54,* pp. 859-874**.**

[6] Siewerdsen J.H., Antonuk L.E., El-M ohri Y., Yorkston J., Huang W., Boudry J.M., Cunningham I.A. (1996), "Empirical and theoretical investigation of the noise performance of indirect detection, active matrix flat- panel imagers (AMFPIs) for diagnostic radiology", *Med. Phys., Vol. 24 (1)*

[7] Cunningham I.A. (1998) "Linear-Systems modeling of parallel cascaded stochastic processes: The NPS of radiographic screens with reabsorption of characteristic X radiation", *Physics of Medical Imaging*, Proc. SPIE 3336.

[8] Jee Kyung-Wook, Antonuk E. Larry, El-Mohri Youcef, Zhao Qihua (2003)," System performance of a prototype flat-panel imager operated under mammographic conditions", *Med. Phys.*, *Vol. 30(7),* pp.1874- 1890.

[9] Kalivas N., Costaridou L., Kandarakis I., Cavouras D., Nomicos C.D., Panayiotakis G.(2002), ″Modeling quantum and structure noise of phosphors used in medical X-ray imaging detectors″, *Nucl.Instr. and Meth. in Phys.Res.*, *Vol. A 490,* pp. 614–629.

[10] Delis H, Spyrou G, Tzanakos G, Costaridou L and Panayiotakis G.(2007) "Evaluating the Figure of Merit in mammography utilizing Monte Carlo simulation", *Nuclear Inst. and Methods in Physics Research A, Vol. 580 (1),* pp.493-496

[11] Alexander L. C. Kwan, John M. Boone, Kai Yang and Shih-Ying Huang (2007), "Evaluation of the spatial resolution characteristics of a cone-beam breast CT scanner", *Med. Phys., Vol. 34 (1),* pp. 275- 281.

[12] Rivetti Stefano, Lanconelli Nico, Campanini Renato, Bertolini Marco, Borasi Gianni, Nitrosi Andrea, Danielli Claudio, Angelini Lidia and Maggi Stefania (2006), "Comparison of different commercial FFDM units by means of physical characterization and contrast-detail analysis", *Med. Phys.*, *Vol.33(11),* pp. 4198-4209.

[13] Aufrichtig R. (1999), "Comparison of low contrast detectability between a digital amorphous silicon and a screen- film based imaging system for thoracic radiography", *Med. Phys, Vol.26 (7),* pp.1349-1358.

[14] Cunningham I.A (2000), *Applied Linear-Systems Theory' in: Handbook of Medical Imaging Vol. 1 Physics and Psychophysics,* Beutel J., Kundel H.L., Van Metter R.L. SPIE, Bellingham.

[15] Zhao W., Ristic G., Rowlands J.A. (2004), "X-ray imaging performance of structured cesium iodide scintillators", *Med. Phys., Vol. 31 (9)*, pp. 2594- 2605.

[16] Cavouras D., Kandarakis I., Nikolopoulos D., Kalatzis I., Kagadis G., Kalivas N., Episkopakis A., Linardatos D., Roussou M., Nirgianaki E., Margetis D., Valais I., Sianoudis I., Kourkoutas K., Dimitropoulos N., Louizi A, Nomikos C., Panayiotakis G.(2005), "Light emission efficiency and imaging performance of Y$_3$Al5O12:Ce(YAG:Ce) powder screens under diagnostic radiology conditions", *Appl. Phys., Vol. B80*, pp. 923-933

[17] Spyropoulou V., Kalyvas N., Gaitanis A., Michail C., Panayiotakis G. and Kandarakis I. (2009), *Modelling the imaging performance and low contrast detectability in digital mammography*, Milos Island, Greece, 22–28 September 2007, JINST, Vol. 4, IOP Publishing and SISSA.

[18] Kyung-Wook Jee, Larry E.Antonuk, Youcef El-Mohri, Qihua Zhao (2003), "System performance of a prototype flat-panel imager operated under mammographic conditions", *Med. Phys., Vol. 30(7),* pp.1874- 1890.

[19] I.A. Cunningham and R. Shaw (1999) "Signal-to-noise optimization of medical imaging systems", *J.Opt.Soc,Am.A, Vol.16,*pp. 621-632.

[20] Lingyun Chen, Chris C. Shaw, Mustafa C. Altunbas, Chao-Jen Lai, and Xinming Liu (2008), "Spatial resolution properties in cone beam CT: A simulation study", *Med. Phys., Vol.35(2),* pp. 724-734.